J Am Oil Chem Soc (2013) 90:273–283
DOI 10.1007/s11746-012-2161-4

ORIGINAL PAPER

Influence of Surfactants on the Rheology and Stability of Crystallizing Fatty Acid Pastes

Prachi Thareja · Anne Golematis · Carrie B. Street · Norman J. Wagner · Martin S. Vethamuthu · Kevin D. Hermanson · K. P. Ananthapadmanabhan

Received: 16 June 2012 / Revised: 23 September 2012 / Accepted: 15 October 2012 / Published online: 1 November 2012

Abstract Complex fluids containing crystallizing fatty acids are important for consumer care products. The key features of these materials are their ability to support their weight under gravity due to the formation of a fatty acid crystal network, and to yield or flow beyond a critical applied strain. In model formulations comprised of two synthetic surfactants and a fatty acid in water, we have shown that the fatty acid crystal network consists of crystal aggregates linked by a non-crystallized mixed fatty acid—surfactant mesophase. We hypothesize that this mixed surfactant—fatty acid mesophase is critical for the macroscopic stability of the formulations. Rheological measurements combined with differential scanning calorimetry (DSC), X-ray scattering, and polarized light microscopy (PLM) measurements show the importance of surfactant loading on the overall stability of the formulations by linking morphology to rheology. Macroscopically homogeneous formulations are realized with 7–10 wt% of fatty acid. Increasing the fatty acid content without adding surfactant leads to inhomogeneous, phase separating formulations. Although both stable and unstable formulations show the presence of a surfactant—fatty acid mixed phase, a critical loading of surfactants is found to be necessary to create macroscopically homogenous formulations. We demonstrate how the rheology, microstructure and the macroscopic stability can be tuned by varying the relative amounts of surfactants and fatty acid.

Keywords Rheology · Crystallization · Time domain nuclear magnetic resonance · Palmitic acid · Stability

Introduction

Pastes containing crystalline solids are often found in food, cosmetics, consumer products and pharmaceuticals [1, 2].

Electronic supplementary material The online version of this article (doi:10.1007/s11746-012-2161-4) contains supplementary material, which is available to authorized users.

P. Thareja · A. Golematis · C. B. Street · N. J. Wagner (✉)
Center for Molecular Engineering and Thermodynamics, Department of Chemical and Biomolecular Engineering, University of Delaware Newark, 150 Academy St, Newark, DE 19716, USA
e-mail: wagnernj@udel.edu

P. Thareja
e-mail: prachi@iitgn.ac.in

A. Golematis
e-mail: annegolematis@gmail.com

C. B. Street
e-mail: cstreet@udel.edu

Present Address:
P. Thareja
Indian Institute of Technology, Gandhinagar, Gujarat, India

Present Address:
A. Golematis
DuPont Analytical Sciences, Wilmington, DE, USA

M. S. Vethamuthu · K. D. Hermanson · K. P. Ananthapadmanabhan
Unilever Research and Development, Trumbull, CT, USA
e-mail: Martin.Vethamuthu@unilever.com

K. D. Hermanson
e-mail: Kevin.Hermanson@unilever.com

K. P. Ananthapadmanabhan
e-mail: KP.Ananth@unilever.com

An underlying feature of these materials is the presence of an internal structure that gives a space filling network capable of supporting its own weight under gravity, i.e., a yield stress [3]. Under an applied critical strain, this space filling network breaks down which causes the material to yield or flow [4]. Therefore, these materials have characteristics of both a solid and a liquid and exhibit a complex, often thixotropic, rheology [5].

Food products with a microstructure comprised of a fat crystal network have been the focus of numerous studies [6, 7]. Central to these studies is the understanding of fat crystallization kinetics and crystal polymorphic transitions using techniques such as time domain nuclear magnetic resonance (TDNMR), Microscopy, time resolved X-ray scattering, differential scanning calorimetry (DSC) and rheology [8–11].

Crystal morphology and aggregation are known to be dependent on waiting time, temperature of crystallization (degree of supercooling) and processing conditions (both thermal and shear history) [12]. Indeed, the influence of the processing history on fat crystallization has been studied for some systems. The effect of shear on the polymorphic transitions of fat in cocoa butter is reported using time resolved X-ray scattering under shear [13, 14]. The rheology of palm oil crystallization under shear has also been explored, complemented by microscopy and time resolved X-ray scattering [15–17]. These studies develop an understanding of structure–property relationships in these materials by correlating the microstructure formed under shear to the observed rheology. Understanding this connection is of value for designing products with desired consistency and appeal.

This paper extends our recent study of a model system designed to emulate a skin care product comprised of a fatty acid crystal network [18]. We have reported the effect of palmitic acid (*n*-hexadecanoic acid) content on the rheology and microstructure of an aqueous solution of synthetic surfactants (9 wt% sodium dodecyl sulfate and 3 wt% cocamidopropyl betaine). Formulations with 12 wt% surfactant and varying amounts of palmitic acid exhibited a high storage modulus ($G' \sim 10^5$ Pa) indicative of a macroscopic space filling crystal network. DSC measurements on crystals separated from the formulation confirmed that the crystals are comprised of palmitic acid [18]. Recent TDNMR measurements led to the hypothesis that these palmitic acid crystals are surrounded by adsorbed layers of hydrated surfactants [19]. X-ray scattering, DSC and polarized light microscopy (PLM) also confirmed the presence of a surfactant-palmitic acid mixed lamellar mesophase in conjunction with crystals [18]. It was proposed that this lamellar phase of mixed surfactant and palmitic acid functions as connective junctions between the crystals. In the absence of this phase, the pure palmitic acid crystals (density of 0.85 g/cm^3) in water do not form a network, but rather, simply cream. This results in macroscopic phase separation. Therefore, the formation and presence of this mixed lamellar phase is critical to the physical stability of the formulations.

The importance of this mixed surfactant-fatty acid gel mesophase is explored further in the research reported herein. We hypothesize that surfactant content plays a significant role in the stability of the formulations. This is tested by reducing surfactant content to 6 wt% (compared to 12 wt% in our previous study), while maintaining the same SDS:cocamidopropyl betaine ratio of 3:1 [18]. Measurements of rheology, X-ray scattering, PLM, TDNMR, DSC and visual observations are combined to resolve the importance of this lamellar phase on formulation stability.

Materials

Sodium dodecyl sulfate (SDS, 9 %, Sigma-Aldrich, CAS# 151-21-3) and palmitic acid (PA, 98 %, Riedel-de Haën, CAS# 57-10-3) were used as supplied. Cocamidopropyl betaine (tegobetaine, CAS# 61789-40-0) provided by Unilever in 28.8 % aqueous form was frozen and lyophilized to obtain the solid tegobetaine used in the formulations. All formulations were prepared with deionized water from a Barnstead nanoPURE water purification system (Thermo Scientific, 18 MΩ). Formulations with constant 4.5 wt% SDS, 1.5 wt% tegobetaine with varying amount of palmitic acid in water were studied and compared to formulations previously studied with constant 9 wt% SDS, 3 wt% CAPB with varying amount of palmitic acid in water. The samples are designated as PA *x*–*y* %., where *x*, denotes the wt% of palmitic acid and *y* denotes the total wt% of surfactant.

Experimental Procedures

Rheology

Crystallization of fatty acids is known to be dependent on both thermal and shear history. Therefore, it is critical to develop a sample preparation and measurement protocol to insure reproducible rheological measurements of model system formulations. To insure mixing and homogeneity, the TA Instruments Starch Pasting Cell (SPC) rheometer tool on an AR-G2 rheometer (TA Instruments) is employed. This tool has been previously employed to study the rheology of palm oil crystallization [20]. The SPC tool consists of a shaft with a mixing blade that can be used to mix the formulation at a specified shear rate. This tool is contained within a Peltier Couette cell that can control the temperature to within ±0.1 °C. Calibration of the tool

Table 1 Sample preparation and rheology measurement protocol for the sample formulations

Step	Action	Time	Shear
1	Combine H_2O and tegobetaine at 70 °C	5 min equilibrium	20 s^{-1} for 5 min
2	Add SDS	5 min equilibrium	20 s^{-1} for 10 min
3	Add PA	15 equilibrium	20 s^{-1} for 30 min
4	Cool at 1 °C/min to 25 °C	45 min	20 s^{-1} while cooling
5	Apply the 3 Pa oscillatory stress at 1 rad/s	18 h	No shear

geometry against rheological standards enables the extraction of accurate and reproducible shear and small amplitude elastic and viscous moduli from the measured torque versus displacement [18]. The formulations were mixed with the blades in a temperature controlled cylindrical cup, thereby providing excellent mixing along with in situ rheological measurements during and after processing all in the same geometry.

Sample Preparation and in Situ Rheology Measurement Protocol

The sample preparation and rheological protocol for measuring the microstructural development is specified in Table 1. The formulations were prepared following a previously reported methodology in the SPC by stepwise addition of tegobetaine, SDS and PA at 70 °C. The formulations were mixed and then cooled to 25 °C while applying a steady shear rate of 20 s^{-1}. At 25 °C, an oscillatory time sweep is performed at a frequency of 1 rad/s in stress control mode to monitor the microstructure development. The applied maximum stress of 3 Pa was shown to provide reliable measurements without disrupting the structure. In this manner the rheological state of the samples could be determined during mixing as well as post mixing within the same cell without destruction or modification of the sample microstructure. Note that testing in standard cone and plate or parallel plate geometries, which requires transfer of the sample from a mixing geometry to this tooling, led to irreproducible results and sample drying; problems avoided through the use of the SPC. The development of both the storage (G') and loss moduli (G'') was monitored to investigate the microstructural evolution with time at 25 °C.

Polarized light Microscopy (PLM)

Microscopy experiments were performed on a Nikon Eclipse TE2000-U microscope. A small amount of sample was placed on a glass slide and then covered with a glass coverslip. This sample preparation method insured a thin layer of sample for ease of visualization. The edges of the coverslip were sealed with a UV curable optical adhesive (Norland Optical Adhesive, Norland Products, Inc., Cranbury, NJ, USA) to minimize water evaporation. Samples were visualized under cross polarizers as crystals and surfactant mesophases exhibit birefringence.

Differential Scanning Calorimetry (DSC)

Time sequence melting profiles of the samples were collected using a Mettler Toledo DSC 1 Star System (Mettler Toledo, USA). For each DSC run, approximately 10–15 mg of sample was hermetically sealed in a 40-µl aluminum pan and was heated at 5 °C/min. The melting temperature T_m was defined as the maximum temperature of the endothermic peak observed during the scan.

X-Ray Scattering

X-ray scattering experiments were conducted on a SAXSess (Anton-Parr), small-angle X-ray scattering system. Samples were placed in a vacuum-tight 1-mm diameter quartz capillary holder, and measured at 25 °C. Cu K_α radiation ($\lambda = 1.54$ Å) was used with a 265-mm sample-to-detector distance. The scattering patterns were collected on a phosphor imaging plate with in the q range 0.05–2.8 $Å^{-1}$. Patterns are normalized to the height of the primary beam signal using the SAXSquant software.

Time Domain Nuclear Magnetic Resonance (TDNMR)

TDNMR measurements were performed on formulations of 12 wt% surfactant with varying palmitic acid content. The procedure for measurements is described in detail elsewhere [19]. Calculations based on equilibrium solids content were used to estimate the amounts of immobile surfactant surrounding the palmitic acid crystals in the formulations.

Solubility

The solubility of palmitic acid in water with 6 wt% surfactant was estimated by preparing a concentration series using the following procedure. Palmitic acid was weighed on weighing paper and transferred to sample vials. The appropriate amounts of stock solutions of 15 wt% SDS in DI water and 15 wt% tegobetaine in DI water, and the required make-up water were added to the sample vials. Each sample had a total mass of 5 g. The samples were then placed in a water bath maintained between 70–80 °C (above the melting point of palmitic acid) for

approximately 4 h. The vials were inverted as needed to insure homogeneity. The samples were then transferred to a water bath maintained at 25 °C. The samples were left in this water bath for 7 days. Digital pictures of the samples in bright field and cross-polarized light were collected to determine the solubility of palmitic acid (supplementary material for [19]). Samples that were mostly clear indicated solubilization of palmitic acid; crystals were apparent in the samples where the amount of palmitic acid exceeded the solubility.

Results and Discussion

To provide insight into the critical role of the surfactant content in the development of yield stress in these formulations the rheological properties were analyzed in terms of the underlying microstructural change during crystallization. The microstructural change was characterized by X-ray scattering, DSC and PLM. We further support our experimental observations with composition calculations derived from recent TDNMR measurements of crystal content of formulations containing 12 wt% surfactant with different amounts of palmitic acid [19].

Rheology

The evolution of the mechanical state of the samples immediately after cooling to 25°C, which defines $t = 0$, is monitored by performing dynamic oscillatory sweep experiments. The time dependence of the rheological properties of the formulations containing 3–7 % palmitic acid (PA) is shown in Fig. 1. In this figure, the complex viscosity ($|\eta^*|$) is plotted for the PA 3–6 % and 5–6 % samples because these samples exhibit predominantly viscous behavior with very low storage modulus values (G' $\sim$ 0.01 Pa). These formulations are observed to be liquid-like when handled, consistent with the observed rheology. There is a mild rise in viscosity with time that slowly decreases with further observation time. However, upon increasing the palmitic acid to 7 wt% (Fig. 1), there is a significant increase in viscosity with time. In this sample, the dynamic viscosity starts at a significantly higher value and, after an induction time and a small dip in modulus, increases rapidly until it plateaus at a viscosity of order 10^5 Pa s. A high dynamic viscosity of this magnitude indicates that the sample has transformed into a solid like paste. Thus, to characterize the PA 7–6 % and samples with a higher palmitic acid loading, the time evolution of the storage modulus (G') is reported.

As shown in Fig. 2, the PA 7–6 % sample shows an initial modulus G′of 2,000 Pa after cooling to 25 °C, which is followed by a slight decrease in modulus with time and

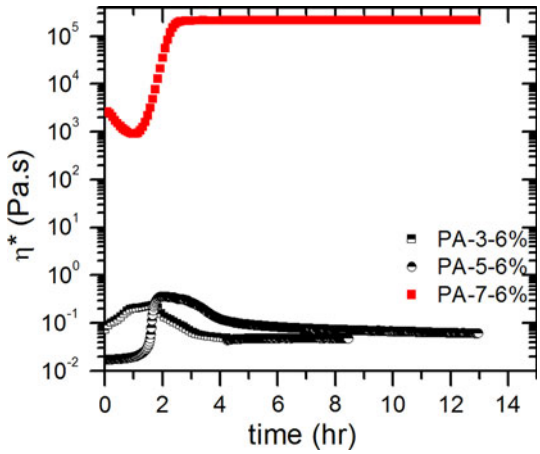

Fig. 1 Dynamic viscosity of formulations with PA 3–7 wt% at 25 °C, oscillatory frequency of 1 rad/s and stress of 3 Pa

then, a significant rise and leveling off to a plateau value of $G'_p \sim 150$ kPa. This plateau value G'_p is observed to remain constant for 18 h in these experiments and is a characteristic of the formation of a macroscopic space filling palmitic acid crystal network, which gives paste like consistency to the formulations. On increasing the palmitic acid content to 18 wt%, G' starts at a slightly higher value and shows a similar, qualitative behavior as for the 7 wt% until it reaches a peak value around 1 h. Note that, as reported previously, the higher palmitic acid content leads to a faster formation of a network [18]. However, unlike the PA 7–6 % formulation, G' peaks and begins to decrease with time. This progressive decrease in G' is a sign that the palmitic acid crystal network is not stable and instead, structural breakdown is observed. This is in contrast to the samples with 12 wt% surfactant reported previously [18], which exhibited a plateau modulus G'_p without decrease at long times. This data are also shown in Fig. 2 for comparison.

Reducing surfactant loading also affects the rate of structural build-up of the network, which is monitored by the measurement of buildup of the elastic modulus. As shown in Fig. 2, the formulation with 6 wt% surfactant and 7 wt% palmitic acid has a much higher initial modulus as compared to its 12 wt% surfactant counterpart, although, the final plateau moduli (G'_p) are comparable. We hypothesize that reducing the surfactant loading reduces the amount of palmitic acid solubilized along with surfactants, thus increasing the concentration of palmitic acid available for crystallization. This provides a greater driving force for crystallization and a more rapid network build up. This effect is not evident at higher palmitic acid concentration (18 wt%). Previous work has demonstrated that significant crystallization already occurs during cooling at these high palmitic acid concentrations [18], which leads to higher moduli upon cooling.

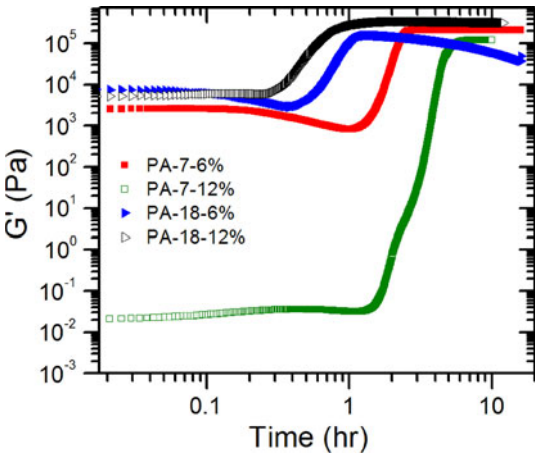

Fig. 2 Comparison of G' versus time for PA 7–6 %, PA 18–6 %, PA 7–12 % and PA 18–12 % formulations at 25 °C, oscillatory frequency of 1 rad/s and stress of 3 Pa

Further rheological characterization of the formulations containing 6 wt% surfactants with varying amounts of PA between 8–11 % show qualitatively the same rheological behavior as the PA 7–6 % sample i.e., a constant G'_p at long times. These data are shown in Fig. 3a. On the other hand, for PA concentrations in the range of 12–20 % the samples show a progressive decrease in G' at long time, similar to PA 18–6 %. This loss of modulus at long times becomes much more pronounced as the palmitic acid loading is increased (Fig. 3b). Visual observation of the samples recovered from SPC at the end of rheological measurements (after 18 h) show that stable formulations are realized with 7–11 wt% of palmitic acid, whereas macroscopic phase separation occurs with higher loading of palmitic acid, as shown in Fig. 3c. This phase separation leads to a homogeneous dense phase separated from a creamed layer by a clear liquid.

Comparison of visual observations of stability with rheology shows that the samples that exhibit a decrease in the plateau storage modulus also undergo visual phase separation. Therefore, in this system two regimes of rheological behavior and macroscopic stability are observed (1) stable formulations that exhibit a constant G'_p and (2) unstable formulations that exhibit a maximum followed by a long time decrease in G' with time. This is summarized in Fig. 3d where the values of G'_p for stable formulations and G' after 10 h (G'_{10hr}) for unstable formulations are compared. To better illustrate the regimes, the results of the visual stability assessment have also been added to this plot. As shown in Fig. 3d, upon increasing the palmitic acid content in the formulation from 7 to 11 wt%, the G'_p value increases until 8 wt% and then shows a decrease with increasing wt% of palmitic acid. A further increase in palmitic acid content in the initial formulation to the range of 11–14 wt% (shaded area in Fig. 3d) leads to an unstable formulation whereby the moduli start to decrease at long times. Further increases in PA loading result in samples that phase separate under gravity. This is in contrast to the formulations with 12 wt% total surfactant, where stable formulations are realized for the entire range of palmitic acid loading of 7–20 wt% [18]. Thus, the surfactant loading is shown to play a critical role in the rheological behavior of the formulations and is related to their macroscopic stability.

Microstructural Characterization

To better understand the microstructural conditions that lead to the stable and unstable regimes, two formulations (7 and 18 wt% PA) were chosen to be studied in more detail.

The characterization of pure palmitic acid crystals provides a baseline for comparison to the model system formulations. As reported in our earlier publication, the pure palmitic acid crystals used in this study appear as thin platelets when observed under a microscope using crossed polarizers [18]. The DSC melting trace of palmitic acid is reported to show an endothermic peak with a melting temperature of 62.7 °C [18]. In X-ray scattering experiments, the palmitic acid crystals show the presence of a peak at q = 0.17 $Å^{-1}$. This corresponds to a spacing of 36.2 Å, which is consistent with the crystal spacing for the α or C form of palmitic acid as reported by us and Verma et al. [18, 21].

To further investigate the microstructural origins of the rheological properties of these formulations, PLM, DSC, and X-ray scattering measurements were performed during the time evolution of the rheological properties at 25 °C (Figs. 4, 5). After cooling to 25 °C and waiting $t = 60$ min, the PA 7–6 % formulation shows the presence of platelet-like crystals and a few Maltese crosses, which indicates the presence of multilamellar vesicles (Fig. 4a). The corresponding DSC melting trace shows a broad endothermic transition around 60–65 °C indicating the presence of crystals containing palmitic acid (Fig. 4d). These crystals continue to grow into long platelet-like crystals with time, as shown in Fig. 4b, c. The corresponding DSC melting trace at long time ($t = 19$ h) shows transitions at 46 °C and 61.2 °C (Fig. 4f). The presence of high aspect ratio platelet-like crystals is concomitant with the behavior of a plateau in G' as shown in Fig. 2. This DSC trace is similar to the system with 12 wt% surfactant, where a fully developed transition with peak at 42 °C along with a small transition at 61 °C is associated with the presence of platelet-like crystals [18].

Prior to phase separation, the PA 18–6 % formulation shows the presence of crystals, which appear bright in the PLM image (Fig. 5a). The corresponding DSC melting

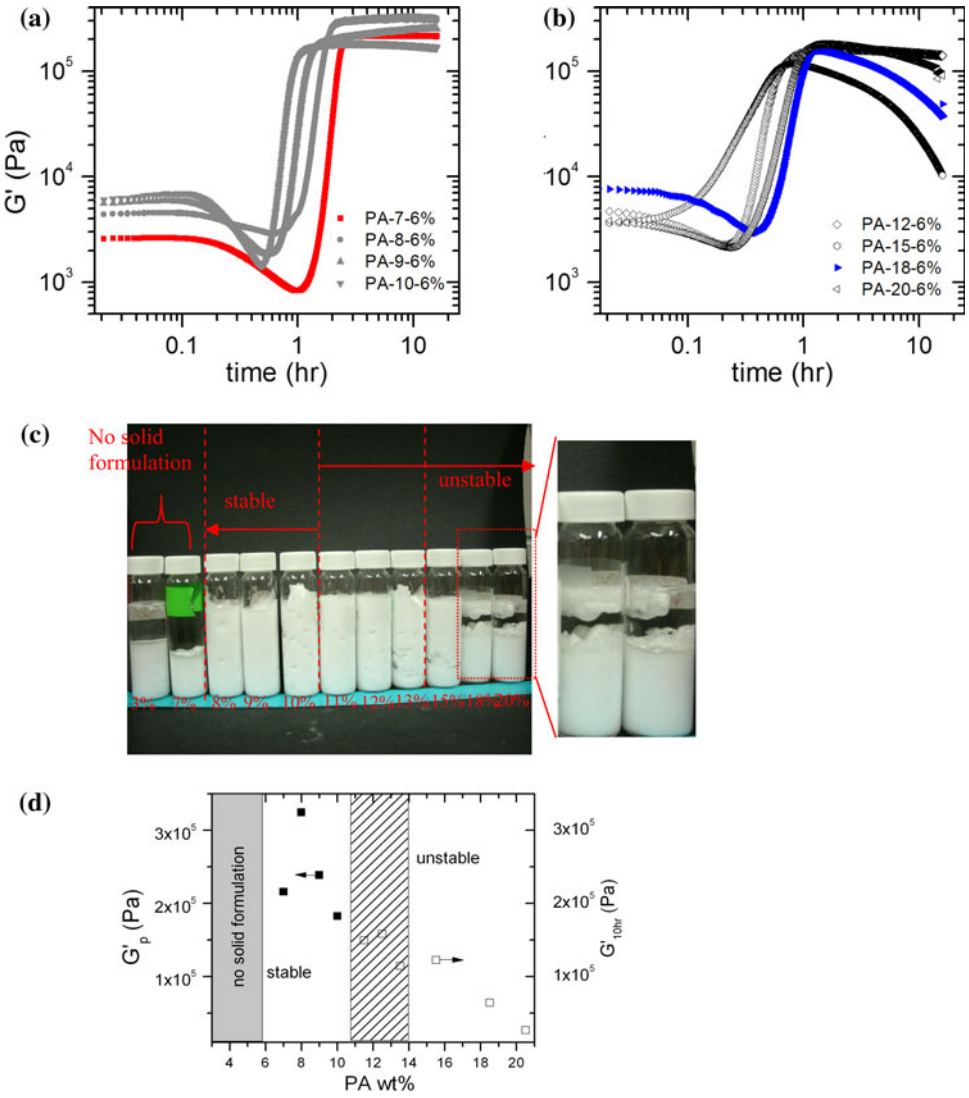

Fig. 3 **a**, **b** Dynamic shear moduli of formulations with 6 wt% surfactant content and varying PA wt% as given at 25 °C, oscillatory frequency of 1 rad/s and stress of 3 Pa. **c** Visual observation of stable and unstable formulations. **d** Plateau modulus G'_p (*filled square*) for stable and longtime elastic modulus G'_{10hr} (*open square*) for unstable formulations with varying PA wt% extracted from **a** and **b**. The *gray region* in **d** shows PA wt% for which no paste like formulations could be formed. The *hashed region* indicates the range of PA wt% for which the formulations begin to become inhomogeneous, eventually leading to macroscopic phase separation

trace shows a sharp transition at 61.3 °C (Fig. 5c). After 140 min, when the PA 18–6 % formulation has phase separated (as shown in Fig. 3c), samples for DSC and X-ray scattering analysis were taken from both the top and bottom portions of the formulation. The crystals continue to grow and form aggregates, as shown in the sample image after 2 h (Fig. 5b). After 140 min the bottom portion of the formulation shows a melting peak at 62 °C and a few very weak transitions near 41–43 °C (Fig. 5d). DSC melting traces indicate that the top is comprised of pure palmitic acid crystals as shown in the inset of Fig. 5d. This is consistent with the creaming behavior as PA floats in water. This is in stark contrast to the formulation with 18 wt% PA and 12 wt% surfactant, which forms macroscopically homogenous samples [18]. The DSC melting trace for this formulation shows the presence of an endothermic peak at 38 °C in addition to the observed peaks at 58 and 62 °C (Fig. 5d).

In the prior study the time sequence DSC melting traces of samples with 12 wt% total surfactant all show the presence of an intermediate DSC peak at approximately 38–42 °C, along with the palmitic acid melting peak (Figs. 4f, 5d). We have shown in our earlier publication, by separating (using a syringe filter to capture the liquid and filter paper to capture the crystals) and characterizing the crystals and the liquid portion of the model system formulation via DSC and X-ray scattering, that the stable formulations with 12 wt% surfactant consist of a mixed surfactant-palmitic acid phase, which shows a DSC melting transition at 38–42 °C, along with a palmitic acid crystalline phase [18]. The mixed mesophase is a swollen lamellar gel phase and is hypothesized to act as linking domains between the crystals. The DSC data for model system formulations with 6 wt% total surfactant lack a clearly defined intermediate peak at approximately 38–42 °C, but show transitions between approximately 40–50 °C in

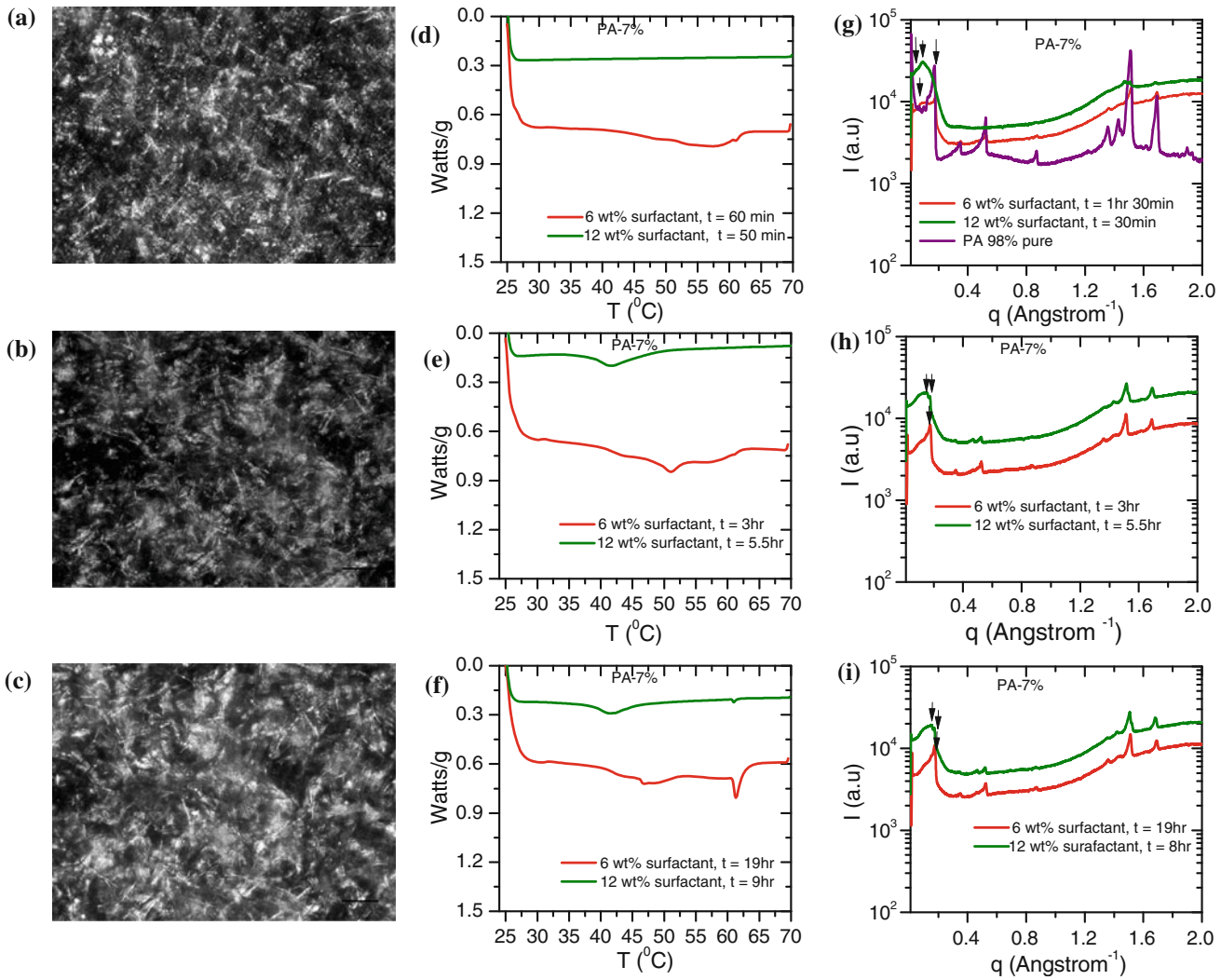

Fig. 4 Time sequence PLM for formulations for PA 7–6 % (**a**), (**b**), (**c**). DSC- (**d**), (**e**), (**f**). X-ray scattering (**g**), (**h**) and (**i**). *Scale bar* represents 100 μm. *Circles* in **a** highlight the presence of Maltese crosses

addition to the clearly defined peak corresponding to the melting of palmitic acid (Figs. 4f, 5d and supplementary material). The magnitude of the palmitic acid melting peak relative to the weak transitions at lower temperatures increases with increasing palmitic acid content. Hence, we observe that increasing the PA loading depletes this mixed mesophase, which is known to be important for network formation. Thus, a sufficient surfactant loading is necessary at each PA loading to form sufficient surfactant-palmitic acid gel phase necessary to link the crystals in a network.

The formation of lamellar gel phases was studied extensively in early publications on industrial monoglycerides [22] and mixtures of surfactants and fatty amphiphiles as stabilizers in dermatological oil-in-water emulsion formulations [23, 24]. These studies report that the gel phase is characterized by alternating bilayers of mixed fatty amphiphiles and ionic surfactant separated by layers of water, forming a viscoelastic network in the continuous phase of oil-in-water dermatological formulations. We observe that, similar to the above mentioned studies, the gel phase acts as a binder between the palmitic acid crystals in our formulations to enable a stable network capable of supporting its own weight under gravity. Therefore, the presence of this gel phase is critical to the macroscopic stability of the formulations.

Crystal Morphology

The samples were diluted to 1:10 crystal:water and examined by optical microscopy. As shown in Fig. 6a, the formulation with PA 7–6 % show thin, platelet-like crystals, whereas the bottom portion of PA 18–6 % formulation shows large aggregates of irregular crystals (Fig. 6b). We have shown in our earlier publication that the shape of the model system formulation crystals transition from longer to shorter aspect ratio plate-like crystals with increase in PA

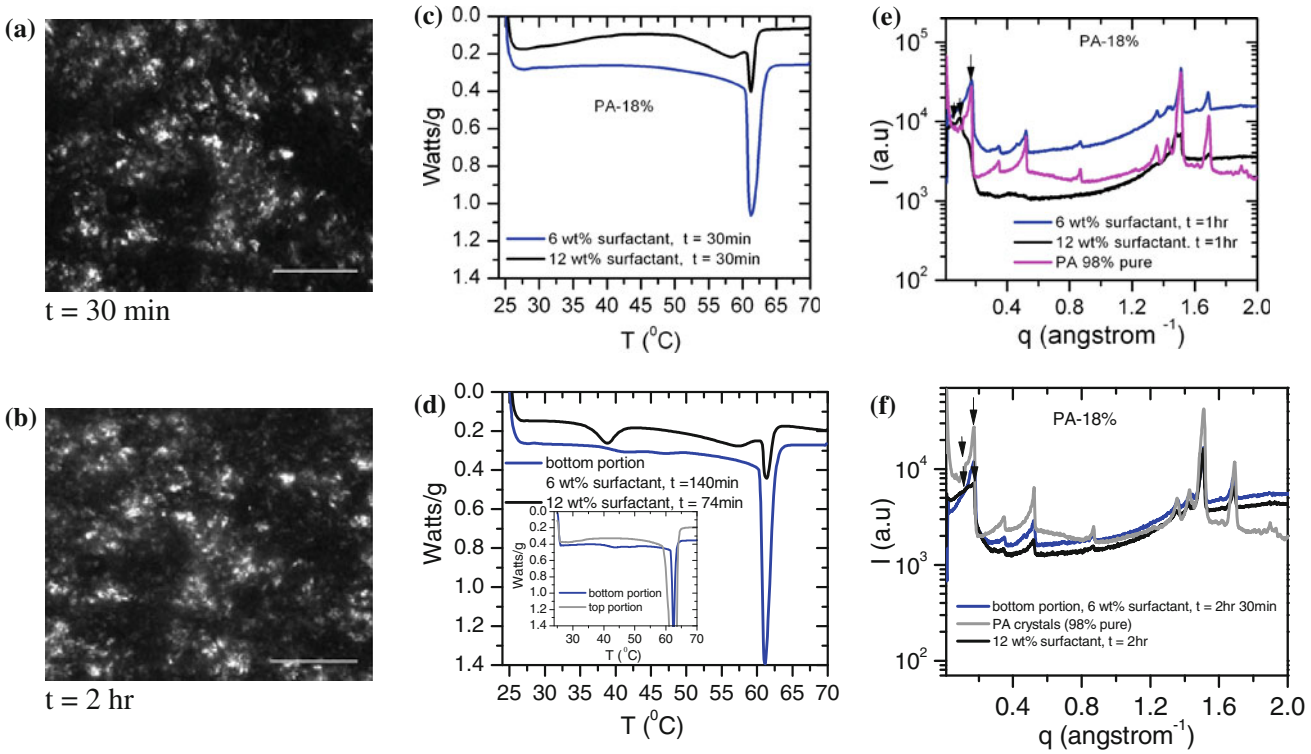

Fig. 5 Time sequence PLM for formulations for PA 18–6 % (**a**), (**b**). DSC (**c**), (**d**). X-ray scattering (**e**), (**f**). *Scale bar* represents 100 μm

content [18] (see Fig. 6c, d). We attribute the change in crystal shape to the change in supersaturation. The effect of supersaturation has been reported to significantly influence the crystal growth rates [25, 26] and will affect the mechanism of nucleation. At 7 wt% palmitic acid, the low degree of supersaturation leads to the slow nucleation and growth of a smaller number of palmitic acid crystals. When the concentration of palmitic acid is increased to 18 wt%, near homogeneous nucleation occurs more rapidly, leading to many more growing crystals. This leads to the rapid formation of many more, smaller crystals rather than the slow growth of fewer large crystals.

In addition to supersaturation effects, the total amount of surfactant plays a role in determining crystal shape in the model system formulations with 6 wt% surfactant. We attribute the change in crystal habit visible between the PA 7–6 % and 18–6 % samples (Fig. 6a, b) to the change in the solubility of palmitic acid in the surfactant solution. While the PA 7–6 % sample (Fig. 6a) bears some resemblance to the PA 7–12 % sample (Fig. 6c), the PA 18–6 % (Fig. 6c) and PA 18–12 % (Fig. 6d) samples differ in appearance. For the PA 18–6 % formulation, the amount of palmitic acid exceeds the amount of surfactant such that it is more favorable to form irregularly shaped crystals with limited surface area exposed to the remainder of the formulation. This change in crystal shape with increase in palmitic acid content in the model system formulations with 6 wt% surfactant may contribute to instability.

Time Sequence X-ray Scattering

The time sequence X-ray scattering for PA 7–6 % is shown in Fig. 4g–i. Initially upon cooling to 25 °C at $t = 50$ min, a peak at 0.0737 $Å^{-1}$ is observed. A characteristic length scale corresponding to the q at which the peak is observed can be calculated using $d = \frac{2\pi}{q}$. We assign the d-spacing of 85 Å to the interlamellar spacing of a mixed surfactantp-fatty acid bilayer. With time (Fig. 4h, i) the low q peaks shift to 0.15 $Å^{-1}$ corresponding to a spacing of 41 Å. In addition, a peak corresponding to the crystal spacing of palmitic acid is also observed at 0.17 $Å^{-1}$(d-spacing of 36 Å). The X-ray data for the bottom portion of PA 18–6 % (Fig. 5e–f) also show the presence of d-spacings of approximately 36 Å and 42 Å. These results are similar to our previous study of formulations with 12 wt% surfactants [18].

The presence of a low q peak (d-spacing approximately 41–42 Å) is a characteristic of these formulations. We have shown in formulations with 12 wt% surfactants that a mixed surfactant-palmitic acid mesophase is formed from a swollen lamellar gel phase that converts into a non-swollen structure with d-spacing of 41–43 Å due to limited

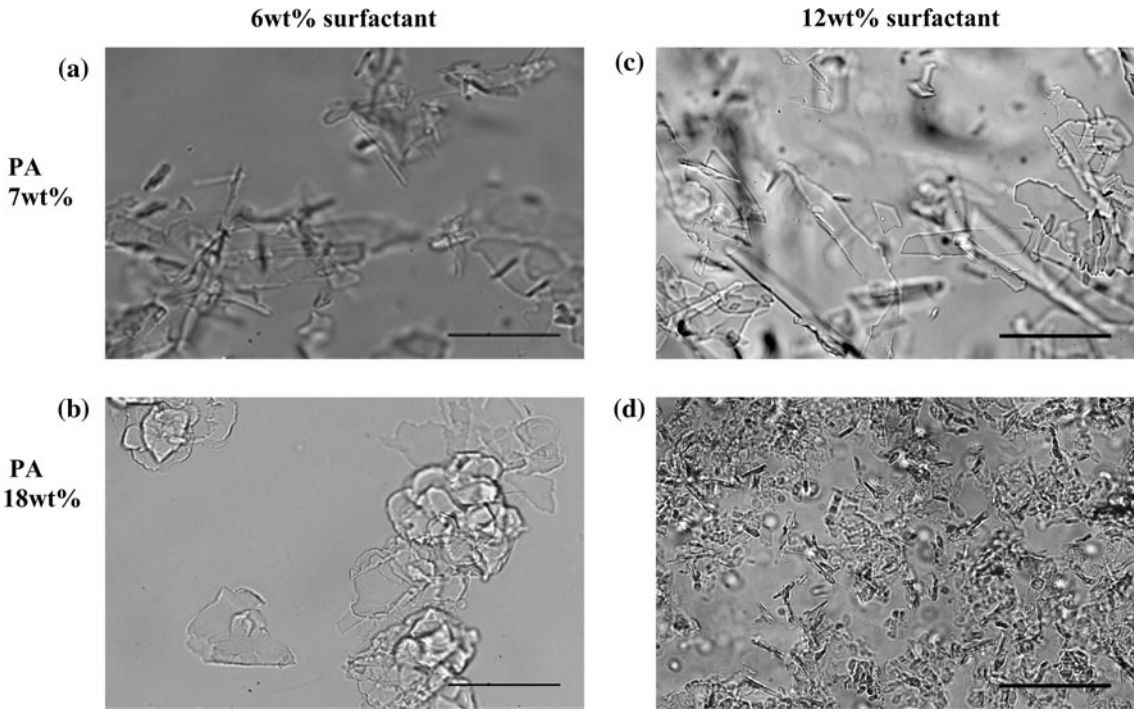

Fig. 6 Diluted crystal images for **a** PA 7–6 % **b** PA 18–6 %. Diluted crystal images for **c** PA 7–12 % **d** PA 18–12 %. *Scale bar* represents 50 μm

Table 2 Summary of time sequence DSC melting traces, X-ray scattering (SAXS)

Sample (wt% PA)	Time (DSC)	DSC transition (°C)	Time (SAXS)	SAXS peak ($Å^{-1}$)	d (Å)
7	60 min	Broad transition 60–65	50 min	0.0737	85.25
7	3 h	51.0	3 h	0.148, 0.174	42.45, 36.11
7	19 h	46.4, 61.3	19 h	0.150, 0.174	41.89, 36.11
Bottom portion 18	30 min	61.3	1 h	0.154, 0.174	40.83, 36.22
Bottom portion 18	140 min	42 (weak), 61.14	2 h 30 min	0.151, 0.173	41.71, 36.22
PA (98 % pure)	–	61.1	–	0.174	36.22

solubility of palmitic acid in the SDS-tegobetaine mixed phase [18]. A summary of DSC and X-ray peak values for the 6 wt% surfactant model system formulations is given in Table 2. The molecular spacings for the model system formulations with 6 and 12 wt% surfactants are comparable. However, the amount of the mixed surfactant-palmitic acid gel phase is critical to the stability, which is addressed in the next section.

TDNMR

Calculations based on recent TDNMR measurements of the solid content of 12 wt% surfactant formulations provide insight into the stability of the 6 wt% surfactant formulations [19]. The measurements show that approximately 2 wt% (based on the total weight) of the palmitic acid resides in the lamellar gel phase for the 12 wt% surfactant formulations. These measurements also show that an immobilized layer of surfactant and water is associated with the crystallized PA in the ratio of approximately 0.3 g of surfactant and water to a gram of crystallized palmitic acid. Thus, the surfactant partitions between adsorption onto the PA crystals and a swollen lamellar phase in the final formulations.

The amount of palmitic acid solubilized with 4.5 wt% SDS and 1.5 wt% tegobetaine was determined by the procedure described in Sect. 3.7 to be approximately 0.3 wt%. This experimentally determined solubility of PA in SDS and tegobetaine is consistent with the recent solubility calculations reported by Tzocheva et al. [27] (see supplementary material for detailed calculations). Calculations analogous to those used for 12 wt% surfactant model system formulations show that the predicted immobile surfactant content (that is, layers of immobile,

Table 3 Calculations of immobilized surfactant with palmitic acid corresponding to the palmitic acid input [19]

Input PA (i_{PA}), wt%	Total input surfactant (i_S), wt%	Predicted immobile surfactant (c_S), wt%
7	6	4.1 ± 0.3
8	6	4.8 ± 0.3
9	6	5.4 ± 0.4
10	6	6
11	6	6.6 ± 0.5
12	6	7.2 ± 0.5
13	6	7.9 ± 0.5
14	6	8.5 ± 0.6
15	6	9.1 ± 0.6
16	6	9.7 ± 0.7
17	6	10.3 ± 0.7
18	6	11.0 ± 0.8

hydrated surfactants that surround the palmitic acid crystals) exceeds the initial surfactant loading for model system formulations with 6 wt% surfactant and PA concentrations greater than 9 wt% (Table 3, calculations in the supplementary material). Thus, in the formulations studies here, at higher PA loadings there is insufficient surfactant present to form the hydrated, immobile surfactant layers that surround the palmitic acid crystals and the surfactant-palmitic acid mixed mesophase. Without a sufficient amount of gel phase to bind the crystals together, the samples macroscopically phase separate due to gravity.

Additionally, in the unstable formulations (PA 15–6 % and 18–6 %), some of the crystals cream while some of the crystals sediment. As noted above, the calculations show that these formulations lack sufficient surfactant to satisfy the amount necessary to surround the palmitic acid crystals, as shown by previous TDNMR measurements [19]. Thus, these formulations have an upper phase comprised of excess pure palmitic acid, as verified by X-ray analysis. This excess pure palmitic acid creams in the unstable formulations because of the lower density of pure PA (0.852 g/ml) than that of the surrounding fluid (mostly water, $\sim$1 g/ml). The densities of the surfactants are greater than the pure palmitic acid and water. Therefore it is reasonable to assume that the sediment contains PA crystals in a network bound together with the swollen surfactant lamellar phase. This is confirmed by the low temperature endotherm in the DSC trace of the bottom phase.

Conclusions

Lowering the amount of surfactant is shown to adversely affect the stability of formulations with high palmitic acid concentration. The characterization using DSC and X-ray scattering shows the presence of palmitic acid crystals along with a mixed surfactant-palmitic acid mesophase in the formulations. However, the unstable formulations do not contain a sufficient amount of the mixed mesophase necessary to bind the crystals together into a homogeneous network. Calculations enabled by recent TDNMR measurements of the immobilized hydrated surfactant layers surrounding the palmitic acid crystals confirm that sufficient surfactant content is required in proportion to the palmitic acid loading to achieve a stable formulation. Thus, exceeding the surfactant capacity by excess loading of palmitic acid leads to a loss of sample homogeneity. In conclusion, we demonstrate that the rheology, microstructure and the macroscopic stability of surfactant, fatty acid mixtures can be tuned by varying the relative amounts of surfactants and fatty acid. These fundamental aspects can be used to enhance the design and shelf life of consumer products.

Acknowledgments Financial support for this work was provided by Unilever, Inc. The authors would like to thank Dr. Steve Sauerbrunn of Mettler Teledo for providing assistance with the calorimetric measurements.

References

1. Coussot P (2005) Rheometry of pastes, suspensions, and granular materials: applications in industry and environment. Wiley-Interscience, Hoboken
2. Coussot P (2007) Rheophysics of pastes: a review of microscopic modelling approaches. Soft Matter 3:528–540
3. Stokes JR, Frith WJ (2008) Rheology of gelling and yielding soft matter systems. Soft Matter 4:1133–1140
4. Stokes JR, Telford JH (2004) Measuring the yield behaviour of structured fluids. J Nonnewton Fluid Mech 124:137–146
5. Mewis J, Wagner NJ (2009) Thixotropy. Adv Colloid Interface Sci 147–48:214–227
6. Heertje I, Lewis DF (1993) Structure and function of food-products—a review. Food Structure 12:343–364
7. Marangoni AG (2005) Fat crystal networks. Marcel Dekker, New York
8. Wiking L, De Graef V, Rasmussen M, Dewettinck K (2009) Relations between crystallisation mechanisms and microstructure of milk fat. Int Dairy J 19:424–430
9. Wright AJ, Scanlon MG, Hartel RW, Marangoni AG (2001) Rheological properties of milkfat and butter. J Food Sci 66: 1056–1071
10. Cebula DJ, Smith KW (1991) Differential scanning calorimetry of confectionery fats—pure triglycerides—effects of cooling and heating variation. J Am Oil Chem Soc 68:591–595
11. Marangoni AG, McGauley SE (2003) Relationship between crystallization behavior and structure in cocoa butter. Cryst Growth Des 3:95–108
12. Litwinenko JW, Rojas AM, Gerschenson LN, Marangoni AG (2002) Relationship between crystallization behavior, microstructure, and mechanical properties in a palm oil-based shortening. J Am Oil Chem Soc 79:647–654

13. MacMillan SD, Roberts KJ, Rossi A, Wells MA, Polgreen MC, Smith IH (2002) In situ small angle X-ray scattering (SAXS) studies of polymorphism with the associated crystallization of cocoa butter fat using shearing conditions. Cryst Growth Des 2:221–226
14. Mazzanti G, Guthrie SE, Sirota EB, Marangoni AG, Idziak SHJ (2004) Novel shear-induced phases in cocoa butter. Cryst Growth Des 4:409–411
15. De Graef V, Dewettinck K, Verbeken D, Foubert I (2006) Rheological behavior of crystallizing palm oil. Eur J Lipid Sci Technol 108:864–870
16. De Graef V, Foubert I, Smith KW, Cain FW, Dewettinck K (2007) Crystallization behavior and texture of trans-containing and trans-free palm oil based confectionery fats. J Agric Food Chem 55:10258–10265
17. De Graef V, Goderis B, Van Puyvelde P, Foubert I, Dewettinck K (2008) Development of a rheological method to characterize palm oil crystallizing under shear. Eur J Lipid Sci Technol 110:521–529
18. Thareja P, Street CB, Wagner NJ, Vethamuthu MS, Hermanson KD, Ananthapadmanabhan KP (2011) Development of an in situ rheological method to characterize fatty acid crystallization in complex fluids. Colloids Surf A: Physiochem Eng Aspects 388:12–20
19. Street CB, Yarovoy Y, Wagner NJ, Vethamuthu MS, Hermanson KD, Ananthapadmanabhan KP (2012) TDNMR study of a model crystallizing surfactant system. Colloids Surf A: Physicochem Eng Aspects 406:13–23
20. de Graef V, van Puyvelde P, Goderis B, Dewettinck K (2009) Influence of shear flow on polymorphic behavior and microstructural development during palm oil crystallization. Eur J Lipid Sci Technol 111:290–302
21. Verma AR (1955) Interferometric and X-ray investigation of the growth of long-chain fatty acid crystals 1. Polymorphism and polytypism in palmitic acid crystals. In: Proceedings of the Royal Society of London Series a-Mathematical and Physical Sciences 228:34–50
22. Krog N, Borup AP (1973) Swelling behavior of lamellar phases of saturated monoglycerides in aqueous systems. J Sci Food Agric 24:691–701
23. Eccleston GM (1986) The microstructure of semi soild creams. Pharm Int 7:63–70
24. Eccleston GM (1997) Functions of mixed emulsifiers and emulsifying waxes in dermatological lotions and creams. Colloids Surf A: Physicochem Eng Aspects 123:169–182
25. Hallett J, Mason BJ (1958) The influence of temperature and supersaturation on the habit of ice crystals grown from the vapour. In: Proceedings of the Royal Society of London Series a-Mathematical and Physical Sciences 247:440–443
26. Sarig S, Eidelman N, Glasner A, Epstein JA (1978) Effect of supersaturation on the crystal characteristics of potassium-chloride. J Appl Chem Biotech 28:663–667
27. Tzocheva SS, Kralchevsky PA, Danov KD, Georgieva GS, Post AJ, Ananthapadmanabhan KP (2012) Solubility limits and phase diagrams for fatty acids in anionic (SLES) and zwitterionic (CAPB) micellar surfactant solutions, J Colloid Interface Sci 369:274–286